

On T2* Magnetic Resonance and Cardiac Iron

John-Paul Carpenter, MB, MRCP*; Taigang He, PhD*; Paul Kirk, MB, MRCP;
Michael Roughton, MSc; Lisa J. Anderson, MD, MRCP; Sofia V. de Noronha, PhD;
Mary N. Sheppard, MD, FRCPATH; John B. Porter, MD, FRCP, FRCPATH; J. Malcolm Walker, FRCP;
John C. Wood, MD; Renzo Galanello, MD; Gianluca Forni, MD; Gualtiero Catani, MD;
Gildo Matta, MD; Suthat Fucharoen, MD; Adam Fleming, BSc; Michael J. House, PhD;
Greg Black, MSc; David N. Firmin, PhD; Timothy G. St. Pierre, PhD; Dudley J. Pennell, MD, FRCP

Background—Measurement of myocardial iron is key to the clinical management of patients at risk of siderotic cardiomyopathy. The cardiovascular magnetic resonance relaxation parameter R2* (assessed clinically via its reciprocal, T2*) measured in the ventricular septum is used to assess cardiac iron, but iron calibration and distribution data in humans are limited.

Methods and Results—Twelve human hearts were studied from transfusion-dependent patients after either death (heart failure, n=7; stroke, n=1) or transplantation for end-stage heart failure (n=4). After cardiovascular magnetic resonance R2* measurement, tissue iron concentration was measured in multiple samples of each heart with inductively coupled plasma atomic emission spectroscopy. Iron distribution throughout the heart showed no systematic variation between segments, but epicardial iron concentration was higher than in the endocardium. The mean±SD global myocardial iron causing severe heart failure in 10 patients was 5.98±2.42 mg/g dry weight (range, 3.19 to 9.50 mg/g), but in 1 outlier case of heart failure was 25.9 mg/g dry weight. Myocardial ln[R2*] was strongly linearly correlated with ln[Fe] ($R^2=0.910$, $P<0.001$), leading to $[Fe]=45.0 \times (T2^*)^{-1.22}$ for the clinical calibration equation with [Fe] in milligrams per gram dry weight and T2* in milliseconds. Midventricular septal iron concentration and R2* were both highly representative of mean global myocardial iron.

Conclusions—These data detail the iron distribution throughout the heart in iron overload and provide calibration in humans for cardiovascular magnetic resonance R2* against myocardial iron concentration. The iron values are of considerable interest in terms of the level of cardiac iron associated with iron-related death and indicate that the heart is more sensitive to iron loading than the liver. The results also validate the current clinical practice of monitoring cardiac iron in vivo by cardiovascular magnetic resonance of the midseptum. (*Circulation*. 2011;123:1519-1528.)

Key Words: heart ■ iron overload ■ magnetic resonance imaging ■ siderosis ■ thalassemia

Transfusion-dependent patients receive ≈20 times the normal intake of iron, which leads to iron accumulation and damage in the liver, heart, and endocrine organs.^{1,2} Although improvements in survival have been achieved over the last 40 years, iron-induced cardiotoxicity remains a leading cause of morbidity and mortality, especially for patients with β-thalassemia major,^{3–6} and once heart failure develops, the prognosis is poor.⁷ Therefore, assessment of myocardial iron is essential clinically, but conventional non-invasive techniques are less than ideal. Neither serum ferritin nor liver iron concentration gives a reliable indication of cardiac iron in cross-sectional studies.⁸ Monitoring ejection

fraction can be useful, but its value is limited by the difficulty of obtaining reproducible longitudinal measurements, the masking of ventricular dysfunction by the basal high cardiac output seen in chronic anemia, and its late occurrence in the disease process. Even more modern contractile measures, such as tissue Doppler imaging, correlate poorly with cardiac iron.⁹ Endomyocardial biopsy is also unreliable for measuring myocardial iron because of sampling error with very small biopsy samples.^{10,11} The need for an alternative noninvasive measurement of myocardial iron led to the development of an optimized cardiac T2* magnetic resonance (MR) technique. Particulate intracellular iron causes shortening of the MR

Received November 11, 2010; accepted January 28, 2011.

From the Royal Brompton and Harefield National Health Service Foundation Trust, London, UK (J.-P.C., T.H., P.K., S.V.N., M.N.S., D.N.F., D.J.P.); National Heart and Lung Institute, Imperial College London, London, UK (J.-P.C., T.H., P.K., D.N.F., D.J.P.); St. George's Hospital National Health Service Trust, London, UK (L.J.A.); University College Hospitals National Health Service Trust, London, UK (M.R., J.B.P., J.M.W.); Children's Hospital Los Angeles, CA (J.C.W.); Università degli Studi di Cagliari, Ospedale Regionale Microcitemie, Cagliari, Italy (R.G.); Ospedali Galliera di Genova, Genoa, Italy (G.F.); Azienda Ospedaliera Brotzu, Cagliari, Italy (G.C., G.M.); Mahidol University, Puttamonthon Nakornpathom, Thailand (S.F.); and University of Western Australia, Perth, Australia (A.F., M.J.H., G.B., T.G.S.P.).

*Drs Carpenter and He contributed equally to this article.

Correspondence to Dudley J. Pennell, MD, FRCP, Royal Brompton and Harefield NHS Trust, Sydney St, London, SW3 6NP, UK. E-mail d.pennell@ic.ac.uk

© 2011 American Heart Association, Inc.

Circulation is available at <http://circ.ahajournals.org>

DOI: 10.1161/CIRCULATIONAHA.110.007641

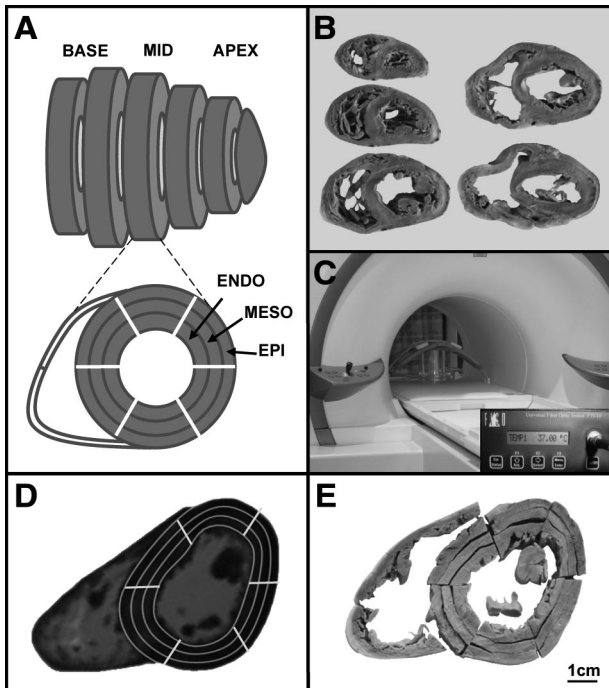


Figure 1. Experimental setup. **A**, Diagram of short-axis cardiac slices showing regions of interest (ROIs). **B**, Set of slices from a single heart. **C**, Slices inside scanner. **D**, Ex vivo cardiac magnetic resonance image with ROIs used to determine T_2^* decay. **E**, Identical slice with segmentation performed to correspond with ROIs used for T_2^* measurement.

relaxation parameter T_2^* (and hence an increase in its reciprocal, R_2^*) owing to microscopic magnetic field inhomogeneity. Myocardial T_2^* is an easily quantifiable, clinically robust, and highly reproducible measurement technique.^{12–14} In the liver, T_2^* correlates well with biopsy iron concentration.^{8,15} Although the relationship between T_2^* and cardiac iron can be inferred from first principles, animal models,¹⁶ and the liver data, there is limited direct information on cardiac calibration of T_2^* in humans,^{17,18} and the inherent limitations associated with endomyocardial biopsy prevent in vivo calibration.¹⁹ We therefore initiated a project to calibrate cardiac T_2^* against chemically assayed tissue iron concentration in ex vivo human hearts and to determine its cardiac distribution.

Clinical Perspective on p 1528

Methods

Patient Characteristics

This project was started in 2003 and completed in 2010, during which time 12 whole human hearts were donated from 5 international centers: University College Hospital (London, United Kingdom), Ospedale Galleria (Genoa, Italy), Children's Hospital of Los Angeles (United States), Azienda Ospedaliera Brotzu (Cagliari, Italy), and Mahidol University (Bangkok, Thailand). All patients were transfusion dependent (10 with β -thalassemia major, 1 with sideroblastic anemia, and 1 with Diamond Blackfan anemia), most having required transfusions from early childhood. The hearts were donated after death or cardiac transplantation for end-stage heart failure. The study protocol was approved by all local research ethics committees, and local consent was obtained in all cases.

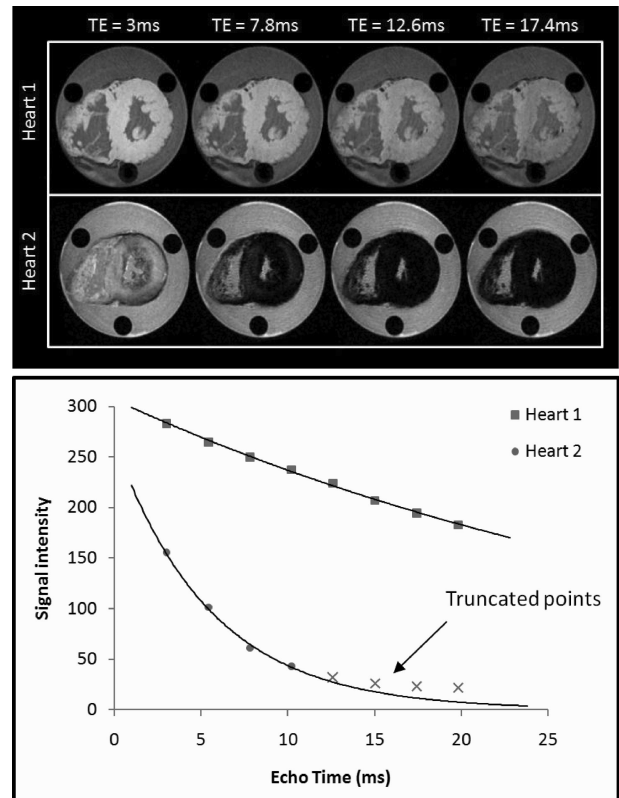


Figure 2. Example of ex vivo cardiac T_2^* scans. Representative images of 2 hearts are shown at increasing echo times (TE) from 3 to 17.4 milliseconds. Heart 1 has normal iron levels and remains bright, whereas heart 2 (which has severe iron loading) shows progressive darkening with increasing echo time. The graph shows signal intensity (arbitrary units) plotted against echo time (milliseconds) for the hearts shown on top. Heart 1 has a shallow decay curve with T_2^* value of >20 milliseconds. Heart 2 has a much more rapid decay with T_2^* <10 milliseconds.

Imaging Protocol and Analysis

We used scientific convention in quoting R_2^* to evaluate relaxation and its relation to iron, R_2^* being the reciprocal of T_2^* . Scans performed on patients pre-mortem are quoted as T_2^* . All hearts were fixed in formalin. Each heart was cut into 4 to 5 slices of 1-cm thickness in the ventricular short axis according to ventricular size (Figure 1A and 1B). The apical cap was not analyzed for R_2^* because of the potential for partial volume effects. All slices were imaged with a 1.5-T MR scanner (Sonata, Siemens Medical Systems, Germany) with a 4-element phased-array coil. Slices were immersed in water in a custom-made container between 2 sheets of Plexiglas and maintained at 37°C throughout imaging (Figure 1C). A multi-echo gradient-echo sequence was used for imaging, and to cover R_2^* values from 25 to 500 seconds^{-1} (T_2^* from 2 to 40 milliseconds), 2 sequences were required. For all hearts, a high-resolution sequence with 16 echoes was used with echo times from 3.1 to 39.1 milliseconds. The parameters were as follows: slice thickness, 5 mm; flip angle, 35° ; matrix, 128×128 pixels; field of view, 160 mm; number of excitations, 2; and sampling bandwidth, 815 Hz per pixel. An additional lower-resolution sequence with a lower minimum echo time was also performed with 12 echoes ranging from 1.21 to 14.9 milliseconds. For this sequence, flip angle was 20° , matrix was 64×64 pixels, and sampling bandwidth was 1955 Hz per pixel. All other parameters were identical. The 2 sequences were compared in 6 ex vivo hearts with a range of R_2^* from 125 to 278 seconds^{-1} (T_2^* from 3.6 to 8.0 milliseconds) and found to agree closely with a coefficient of variation of 5.1%. Care was taken to orientate each slice, including photography, to ensure reliable identification of

Table 1. Patient Characteristics and Clinical Information

Patient	Sex	Diagnosis	Death or Cardiac Transplantation	Age at Death or Transplantation, y	Cause of Death or Indication for Transplantation	LV [Fe] (Mean±SD), mg/g dw	Variability of [Fe], CoV %	Global Myocardial T2* (Mean±SD), ms	Total Estimated Units Transfused	Age Started Chelation, y	Compliance
1	M	TM	Death	46	Ischemic stroke (no cardiac failure)	0.38±0.13	21.1	44.4±5.3	1584	6	Excellent
2	F	SA	Death	62	Cardiac failure	8.20±1.44	15.9	4.7±0.6	2000	42	Good
3	M	TM	Death	10	Cardiac failure	9.50±1.88	9.2	3.7±0.6	170	N/A*	N/A
4	F	TM	Death	15	Cardiac failure	25.9±10.3	17.6	2.0±0.4	288	N/A†	N/A
5	F	TM	Death	20	Cardiac failure	7.74±1.51	16.4	3.6±0.5	432	6	Poor
6	M	TM	Transplant	23	Cardiac failure	3.63±0.82	18.0	8.0±1.0	765	10	Not known
7	M	TM	Transplant	24	Cardiac failure	3.38±0.53	10.0	7.7±1.2	528	6	Good
8	M	TM	Transplant	21	Cardiac failure	5.87±1.0	9.5	4.4±0.6	500	4	Not known
9	F	TM	Transplant	31	Cardiac failure	8.78±1.88	10.5	3.9±0.6	624	7	Poor
10	M	TM	Death	24	Cardiac failure and mucormycosis	5.64±1.36	17.3	5.8±1.4	660	10	Poor
11	M	TM	Death	44	Cardiac failure	3.19±1.02	26.6	12.3±2.6	1209	18	Poor
12	M	DBA	Death	22	Cardiac failure and pneumonia	3.91±0.86	10.1	8.8±1.8	442	10	Poor

LV indicates left ventricle; dw, dry weight; [Fe], myocardial iron concentration; CoV, coefficient of variation; TM, β -thalassemia major; SA, sideroblastic anemia; DBA, Diamond Blackfan anemia; and N/A, not applicable (patients 3 and 4 did not receive iron chelation therapy).

*Died in 1964.

†Died in 1972.

anatomy and wall segmentation for colocalization of R2* and chemically assayed iron concentration.

For the measurement of R2*, each slice was analyzed with 18 regions of interest (ROIs) of 6 radial sectors of 60° each and 3 layers: outer (epicardial), inner (endocardial), and intermediate (mesocardial; Figure 1D). The attachment of the right ventricular (RV) wall to the left ventricle (LV) was used to define the septum.²⁰ R2* was measured from each ROI with dedicated software (Thalassaemia Tools, Cardiovascular Imaging Solutions, London, UK) using a truncation model to account for background noise, as has been validated previously (Figure 2).²¹ Analysis of the 12 echo sequence was required only for heart 4, which was extremely heavily iron loaded (R2*, 500 seconds⁻¹; T2* 2.0 milliseconds). In all other cases, the 16-echo sequence was used for analysis.

Quantification of Myocardial Iron

After R2* cardiac MR was completed, each short-axis slice was cut into 6 sectors of 60° each, and then each sector was subdivided into 3 transmural layers (18 LV samples; Figure 1E). For each short-axis slice, 2 samples were also taken from the RV free wall (20 myocardial samples per slice). Additional samples were taken from the right (3) and left (3) atria, the interatrial septum (1), and each of the valves (4). For the LV myocardial R2* calibration analysis, all LV samples were directly compared with the cardiac MR R2* scan. For the segmental analysis of the distribution of myocardial iron, we used the American Heart Association/American College of Cardiology 16-segment model.²⁰ Three myocardial slices from each heart were used for this analysis: the midventricular, apical, and basal slices, as per the model. Each segment comprised the full transmural extent of myocardium. To match the apical slice to 4 segments as dictated in the 16-segment model, the 2 apical-septal sectors were analyzed together and the 2 apical-lateral sectors were analyzed together. The wet weight of each piece of tissue was recorded after excess formalin was discarded. Samples were then freeze-dried, and the dry weight (dw) was recorded immediately after removal from the lyophilizer. After acid digestion, iron measurement was performed with inductively coupled plasma atomic emission spectroscopy. The iron concentrations in samples of NIST human liver standard 4352 were used as quality controls for inductively coupled plasma atomic emission spectroscopy analysis.

Effect of Time in Formalin Fixation on R2* Measurement and Iron Concentration

Because the fixed hearts had been stored for various lengths of time, the effect of formalin on MR relaxation and iron loss over time was

studied. One myocardial slice was analyzed at repeated intervals up to a total of 566 days (12 scans in total). Myocardial tissue from an apical slice not included in the segmental analysis was used to assess whether there was any leaching of iron from the myocardium into formalin over time. This 7.35-g sample was preserved in 280 mL of 10% neutral buffered formalin (pH 7.0). At repeated intervals up to 600 days, small (1 mL) aliquots of formalin were taken for analysis of the iron content of the solution. The initial iron concentration in this tissue sample was estimated from immediately adjacent areas of myocardium in the same apical slice.

Premortem and Postmortem Scans

Three of the patients had clinical T2* scans shortly before death on the same scanner (Sonata) used for the ex vivo scanning. Imaging was performed with a single-breath-hold 8-echo T2* sequence, as previously described (range of echo times, 2.6 to 16.74 milliseconds; slice thickness, 10 mm; flip angle, 20°; matrix, 128×256 pixels; field of view, 400 mm; and sampling bandwidth, 815 Hz per pixel).¹³ The anatomic appearance of the slice (papillary muscle position, trabecular pattern, and distance from apex) was used to achieve as precise a correlation as possible between premortem and postmortem scans, allowing direct comparison of T2* values. Two midventricular short-axis slices were imaged, which gave 12 myocardial ROIs for comparison (2 slices, 2 septal sectors, and 3 transmural layers).

Statistics

For each distribution analysis, 1 ROI was defined as the reference region, and differences in tissue iron content throughout the heart against this region were assessed with mixed-model linear regression. The null hypothesis was that there was no difference in iron concentration between segments, layers, or slices. For each analysis, the ROIs were entered as fixed effects so that differences between regions could be estimated. Patients were entered as random effects because testing for differences between individual patients was not of interest. To account for the repeated measurements from each heart, all samples from each individual heart were nested for analysis. R2* was compared with iron concentration by linear regression. The degree of heterogeneity of iron concentration and R2* for each heart was evaluated by calculating the coefficient of variation of iron concentration across all samples. All data were analyzed with STATA version 10.1 (Stata Corp, College Station, TX). Mixed-model linear regression analysis was performed with the "xtmixed" command within STATA. The "regress" command was used for standard linear regression. A value of $P < 0.05$ was used to define a significant difference.

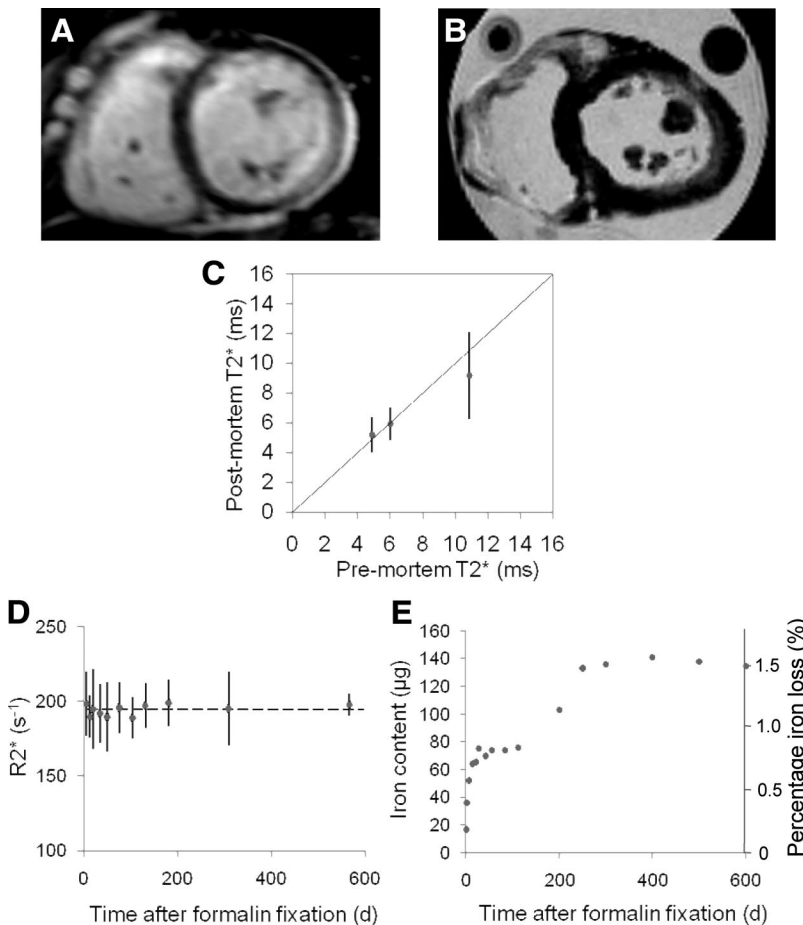


Figure 3. Premortem and postmortem scans. A premortem midventricular slice (A) and the corresponding postmortem slice (B) of the same heart at the same position. C, Relationship between premortem and postmortem T2* values measured from corresponding regions of interest in the midventricular septum. Error bars represent SDs, and the line of identity is given. D, R2* values measured from a single myocardial slice stored in formalin over a prolonged duration showing no significant change in R2*. The dashed line represents mean R2* (194.4 seconds⁻¹), and error bars are \pm SD. E, Iron content of the formalin solution in which a piece of myocardial tissue was stored, showing an initial rapid increase in iron that reaches a plateau after the first 300 days. There is an early and a late plateau, possibly suggesting a 2-stage process of iron release; however, no further iron appears to be lost after the first 300 days. Note that T2* (decay constant in milliseconds) is in widespread use for clinical iron assessment and is shown for the patient scan results but that R2* (transverse relaxation rate in seconds⁻¹) has been used to compare measurements in postmortem hearts because it has a more linear relation to iron concentration.

Results

Patient Characteristics

Twelve hearts were donated, 8 from patients who died and 4 from patients undergoing cardiac transplantation for end-stage heart failure. End-stage heart failure was the cause of death in 7 of the 8 patients who died, but 1 patient died of an ischemic stroke at 46 years of age with a history of excellent compliance to chelation therapy and no cardiac complications (apart from a transient episode of atrial fibrillation at 21 years of age). Table 1 summarizes the clinical information for each patient.

Premortem and Postmortem Scans

Three patients underwent both premortem and postmortem T2* scans. The mean \pm SD time between cardiac MR scan and death was 26 ± 13.3 days (range, 11 to 35). There was no significant difference in T2* between scans. T2* premortem was 4.89 ± 1.30 , 6.01 ± 0.81 , and 10.87 ± 2.34 milliseconds versus 5.21 ± 0.43 milliseconds ($P=0.28$), 5.94 ± 0.90 milliseconds ($P=0.84$), and 9.20 ± 2.22 milliseconds ($P=0.21$) postmortem for pairwise comparison of the septal ROIs in hearts 2, 10, and 11, respectively (Figure 3A through 3C).

Effect of Time in Formalin on R2* Measurement

For the single short-axis slice that was scanned at repeated intervals, there was no significant change in R2* value, even after 18 months' storage in formalin (Figure 3D). Mean R2*

for all sectors was 198.4 ± 21.5 seconds⁻¹ at day 6 and 197.7 ± 7.3 seconds⁻¹ at day 566 ($P=0.93$).

Loss of Iron From Stored Myocardial Samples

The iron content of the formalin solution in which a piece of myocardial tissue had been stored over a period of 600 days is shown in Figure 3E. The average iron concentration of adjacent myocardial tissue was 1.21 mg/g wet weight, corresponding to a total of 8.91 mg iron in the 7.35-g wet weight sample. The iron concentration of the solution increased rapidly over the first 30 days after formalin fixation with a further subsequent rise, but thereafter stabilized to reach a plateau of ≈ 480 μ g/L after 300 days, equating to a loss of 135 μ g ($\approx 1.5\%$) of the total iron from the myocardial tissue.

Myocardial Iron Samples: Overall Summary

The mean \pm SD weight of all samples in the iron analysis was 1001 ± 620 mg. Iron concentration in all samples ranged from 0.09 to 78.64 mg/g dw. The myocardial iron concentration ranged from 0.18 to 53.4 mg/g dw. The mean \pm SD ratio of dry to wet iron concentration in the myocardium was 5.04 ± 0.9 and was independent of iron concentration. One heart had exceptionally high levels of iron, and in view of the possibility that this heart could bias the results, all further analysis is presented separately for this outlier heart. The coefficient of variation of iron for myocardial samples ranged from 9.2% to 26.6% per heart with a mean of 15.2% (Table 1).

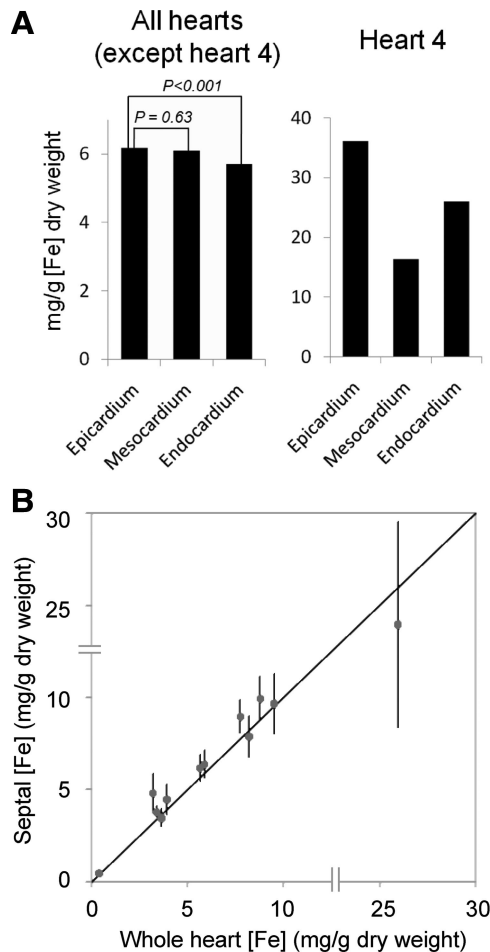


Figure 4. Myocardial iron distribution. **A**, Histogram showing transmural gradient across the left ventricular myocardium; **B**, Graph of midseptal iron concentration vs mean whole-heart iron concentration for each of the 12 hearts (data points are plotted against the line of identity, and error bars are \pm SD of the septal samples). The double lines across each axis represent a discontinuity in the scale between 15 and 25 mg/g for illustrative purposes.

Distribution of LV Iron

With all hearts considered together (except for heart 4, the most heavily iron-loaded heart), a gradient of iron was found in the transmural layers of the LV myocardium with the greatest concentration in the epicardium, an intermediate level in the mesocardium (-1.1% ; $P=0.63$), and the lowest level in the endocardium (-7.5% ; $P=0.001$; Figure 4A and Table 2). No statistically significant systematic variations in iron concentration were observed between the different AHA segments. To examine for variation in larger regions of the LV, an analysis was also performed of variation in iron concentration of whole walls of the LV (inferoseptal, anteroseptal, anterior, anterolateral, inferolateral, and inferior) encompassing all segments from base to apex, which again showed no significant systematic variation of mean iron concentration. A further analysis comparing the whole basal, midventricular, and apical slices also failed to show any significant systematic variation in mean iron concentration. The most heavily iron-loaded heart (heart 4) had very high iron concentration in the epicardium (36.1 mg/g dw), with an intermediate level in the endocardium (-28.0%) and the lowest level in the mesocardium (-54.7% ;

Figure 4A and Table 2). There was no systematic variation in mean iron concentration between the different LV segments or from base to apex.

Septal Iron Compared With Global Cardiac Iron

Iron concentration measured in the midseptal slice was highly representative of global iron (Figure 4B). Regression analysis showed a slope indistinguishable from 1 (1.06; 95% confidence interval [CI], 0.83 to 1.29) and an intercept indistinguishable from 0 (0.04; 95% CI, -1.57 to 1.66). The mean \pm SD percentage difference between midseptal and global iron concentration was $10.5 \pm 13.4\%$.

Distribution of Iron in the RV, Atria, and Valves

Excluding the most heavily iron-loaded heart (heart 4), all RV, atrial, and valve samples showed lower iron levels compared with global LV iron (apart from the anterior left atrial wall where only a borderline difference was observed). The RV wall had up to 21.9% less iron ($P<0.001$). Compared with the mean global LV iron concentration, the left atrial iron concentration was up to 28.1% lower ($P<0.001$) and right atrial iron was up to 57.0% lower ($P<0.001$). All 4 cardiac valves showed low iron concentrations that were up to 74.4% lower than in the LV ($P<0.001$). Heart 4 showed a consistently higher level of iron in the atrial and valve samples but no difference between LV and RV iron (Table 3).

Relation of R2* to Tissue Iron Concentration

Because of the very high level of iron in the most severely overloaded heart (heart 4), measurement of R2* might be underestimated. Therefore, the results of the MR relaxation calibration are presented twice, first including and then excluding this heart. A total of 1006 tissue samples and their corresponding ROIs were used for iron and R2* assessment, with 84 ROIs (8.3%) being excluded from the R2* analysis because of imaging artifact caused predominantly by cuts made at autopsy. A curvilinear relation between R2* and cardiac iron concentration was observed (Figure 5A and 5B). A similar curvilinear relation was shown when mean global whole-heart iron was plotted against R2* (Figure 5C and 5D). The strongest linear correlation was found (all hearts) by plotting $\ln R2^*$ and $\ln [Fe]$ ($R^2=0.910$, $P<0.001$) with a slope of 0.745 (95% CI, 0.729 to 0.760) and intercept of 3.896 (95% CI, 3.868 to 3.924; Figure 5E). There was almost no difference in this calibration result when heart 4 was excluded ($R^2=0.898$, $P<0.001$; slope, 0.754 [95% CI, 0.737 to 0.772]; intercept, 3.884 [95% CI, 3.855 to 3.913]). Using this calibration in all hearts, we can express the relation between R2* and by the following formula (where myocardial [Fe] is measured in milligrams per 1 g dw and R2* is measured in seconds⁻¹): $[Fe]=0.00985 \times (R2^*)^{1.22}$.

R2* measured in the midseptal slice was highly representative of whole-heart mean R2* (Figure 5F). Regression analysis showed a slope indistinguishable from 1 (0.97; 95% CI, 0.82 to 1.13) and an intercept indistinguishable from 0 (0.33; 95% CI, -0.73 to 1.38). The mean \pm SD percentage difference between midseptal and global R2* was $2.8 \pm 7.3\%$. The relation of septal R2* and T2* with whole-heart iron concentration is shown in Figure 6.

Table 2. Distribution of Iron Throughout the Left Ventricular Myocardium

LV Region of interest	All Hearts (Excluding Heart 4)				Heart 4 Alone			
	[Fe], mg/g	Lower 95% CI	Upper 95% CI	<i>P</i>	[Fe], mg/g	Lower 95% CI	Upper 95% CI	<i>P</i>
Epicardium (reference)	6.17	4.65	7.69	Ref	36.10	31.58	40.62	Ref
Mesocardium (Δ)	-0.07	-0.34	0.20	0.63	-19.75	-21.71	-17.79	<0.001
Endocardium (Δ)	-0.46	-0.73	-0.19	0.001	-10.11	-12.75	-7.46	<0.001
Global LV (reference)	6.01	4.30	7.72	Ref	26.15	23.31	28.99	Ref
Basal								
1 Ant (Δ)	-0.37	-1.30	0.56	0.43	1.12			
2 Ant-sep (Δ)	0.09	-0.84	1.02	0.85	-7.31			
3 Inf-sep (Δ)	-0.27	-1.20	0.66	0.57	-6.59			
4 Inf (Δ)	-0.41	-1.34	0.52	0.39	5.26			
5 Inf-lat (Δ)	-0.14	-1.07	0.79	0.77	-4.09			
6 Ant-lat (Δ)	0.38	-0.55	1.31	0.43	-2.99			
Mid								
7 Ant (Δ)	0.03	-0.90	0.96	0.94	4.39			
8 Ant-sep (Δ)	0.50	-0.43	1.43	0.29	3.05			
9 Inf-sep (Δ)	0.59	-0.34	1.52	0.22	-1.33			
10 Inf (Δ)	-0.01	-0.94	0.92	0.98	-0.67			
11 Inf-lat (Δ)	0.02	-0.91	0.95	0.97	2.23			
12 Ant-lat (Δ)	0.43	-0.50	1.36	0.37	1.06			
Apical								
13 Ant (Δ)	0.08	-0.85	1.01	0.87	4.88			
14 Sep (Δ)	-0.29	-1.22	0.64	0.54	-4.43			
15 Inf (Δ)	-0.12	-1.05	0.81	0.81	8.57			
16 Lat (Δ)	-0.50	-1.43	0.43	0.29	3.69			
Global LV (reference)	5.99	4.28	7.71	Ref	26.15	23.31	28.99	Ref
Anterior (Δ)	-0.07	-0.93	0.78	0.87	3.46	-5.30	12.23	0.39
Anterolateral (Δ)	0.16	-0.70	1.01	0.72	-0.36	-8.30	7.58	0.93
Inferolateral (Δ)	-0.06	-0.91	0.80	0.89	1.56	-6.38	9.50	0.69
Inferior (Δ)	-0.16	-1.02	0.69	0.71	4.39	-3.31	12.09	0.26
Inferoseptal (Δ)	-0.06	-0.92	0.79	0.89	-3.93	-7.39	-0.48	0.28
Anteroseptal (Δ)	0.20	-0.66	1.05	0.65	-5.11	-8.29	-1.93	0.16
Apical (Δ)	0.27	-0.55	1.10	0.51	1.99	-4.41	8.40	0.49
Mid (Δ)	-0.17	-1.00	0.66	0.69	0.44	-7.18	8.06	0.88
Basal (Δ)	-0.11	-0.93	0.72	0.80	-2.43	-9.30	4.44	0.40

LV indicates left ventricular; CI, confidence interval; and [Fe], myocardial iron concentration. The differences in iron concentration (Δ) are compared against the mean [Fe] dry weight for a reference (ref) region. American Heart Association segments are numbered and labeled as follows: ant, anterior; sep, septum; lat, lateral; and inf, inferior.

Discussion

This is the first report of a series of human hearts that have undergone both MR relaxometry and quantitative iron studies for distribution and calibration purposes. The results of the distribution analysis show no systematic variation of iron concentration between all 16 myocardial segments, the 6 myocardial walls, and the 3 short-axis slices from base to apex. However, systematically higher iron concentration was present in the epicardium. The midventricular septal iron concentration was highly representative of global iron concentration, and midventricular septal R2* was highly representative of global R2*.

Studies dating from the mid-1950s have assessed myocardial iron loading in postmortem human hearts using various techniques, including histological grading of iron-positive myocytes, electron microscopy, and analysis of elemental iron by flameless atomic absorption spectroscopy.^{11,22–27} Our results are in broad agreement with the previously published studies, which have observed a similar transmural gradient of myocardial iron. Two autopsy studies have attempted to quantify regional variation,

but no definite pattern has emerged,^{17,22} and this is the first comprehensive study of regional variation.

Cardiac MR studies have reported that some β -thalassemia major patients have a heterogeneous pattern of cardiac iron distribution as measured by in vivo T2*, although this heterogeneity lessens with increased iron concentration.^{28,29} Myocardial T2* in vivo, however, may be confounded by a number of factors, including magnetic susceptibility artifact and measurement error.³⁰ In view of the problems with artifact in vivo, it has been recommended that the measurement of T2* be restricted to a full-thickness septal ROI.⁸ There has been debate recently about the use of this septal ROI for predicting whole-heart iron,²⁹ but our results validate this approach given that both iron and R2* measured in the midseptum are highly representative of their respective global myocardial value.

The results of the calibration analysis of myocardial MR relaxometry against absolute iron concentration are of considerable clinical interest. Heart R2* provided a robust ($R^2=0.910$) calibration against chemically assayed cardiac

Table 3. Distribution of Iron in the Right Ventricle, Atria, and Valves

Region of Interest	All Hearts (Excluding Heart 4)				Heart 4 Alone			
	[Fe], mg/g	Lower 95% CI	Upper 95% CI	<i>P</i>	[Fe], mg/g	Lower 95% CI	Upper 95% CI	<i>P</i>
RV								
Global LV [Fe] (reference)	5.98	4.52	7.45	Ref	26.15	23.31	28.99	Ref
RV Posterior (Δ)	-1.26	-1.75	-0.78	<0.001	2.55	-3.86	8.96	0.68
RV Anterior (Δ)	-1.31	-1.80	-0.83	<0.001	10.50	5.51	15.50	0.10
Apical (Δ)	-0.98	-1.57	-0.39	0.001	6.73	6.59	6.95	0.38
Mid (Δ)	-1.43	-2.02	-0.84	<0.001	7.16	-0.69	15.00	0.35
Basal (Δ)	-1.45	-2.04	-0.86	<0.001	5.69	-10.07	21.45	0.46
Atria and valves								
Global LV [Fe] (reference)	5.98	4.57	7.39	Ref	26.15	23.31	28.99	Ref
LA anterior (Δ)	-0.78	-1.64	0.09	0.080	45.92			
LA posterior (Δ)	-1.68	-2.59	-0.76	<0.001	13.26			
LA lateral (Δ)	-1.11	-1.98	-0.24	0.013	30.81			
Atrial septum (Δ)	-2.99	-3.86	-2.12	<0.001	20.81			
RA anterior (Δ)	-3.28	-4.15	-2.41	<0.001	34.22			
RA posterior (Δ)	-3.41	-4.28	-2.54	<0.001	22.17			
RA lateral (Δ)	-3.09	-3.95	-2.22	<0.001	23.39			
Aortic valve (Δ)	-4.45	-5.57	-3.33	<0.001	42.60			
Mitral valve (Δ)	-4.37	-5.23	-3.50	<0.001	52.49			
Pulmonary valve (Δ)	-4.33	-5.45	-3.21	<0.001	41.12			
Tricuspid valve (Δ)	-4.40	-5.26	-3.53	<0.001	52.35			

[Fe] indicates myocardial iron concentration; CI, confidence interval; RV, right ventricle; LV, left ventricle; Ref, reference; LA, left atrial; and RA, right atrial. The differences in iron concentration (Δ) are compared against the mean LV [Fe] dry weight.

iron in the present study. Our statistical analysis demonstrated that this relationship was curvilinear. Previous investigators have described a linear relationship between R2* and iron concentration, but these studies had fewer observations and a more limited range of measurement.¹⁷ Although R2* underestimation may occur at high iron concentrations if initial echo times are too long, a minimum echo time of 1.2 milliseconds should have been adequate to capture even the most heavily loaded samples. In addition, we found little calibration differences if heart 4 was included or excluded. For clinical purposes, for which T2* is typically the result quoted for patients with suspected cardiac iron overload, the calibration equation can be rewritten using $T2^* = 1000/R2^*$ when the units of T2* are expressed in milliseconds and R2* in seconds⁻¹: $[Fe] = 45.0 \times (T2^*)^{-1.22}$.

Although direct comparison across species should be done with caution, our results are comparable to R2* measurements in a gerbil model of severe iron loading in which tissue iron concentration was measured from fresh, unfixed tissue.¹⁶ Proton relaxivity is known to be temperature dependent, and in phantom studies, T2* falls by up to 1.5% per 1°C.³¹ We scanned all hearts at a constant 37°C, which may account for the consistency of our pre-mortem and post-mortem heart measurements. The hearts in this study had been stored in formalin, and there was concern that this could affect the measurement of T2* and iron concentration. In agreement with previous work, we found only minor leaching of iron from myocardial tissue into the formalin solution and very little variation in the measured T2* over time.³²

The iron values obtained from our study are of considerable interest in terms of the level of cardiac iron concentration that is

associated with iron-related death and cardiac disease, an issue that has hitherto been little explored. One previous study reported the normal myocardial iron concentration to be 0.34 mg/g dw (range, 0.29 to 0.47 mg/g dw).³³ The 1 heart we studied from a patient who died of a stroke with no evidence of heart disease and a normal myocardial T2* had a global iron concentration of 0.38 mg/g dw, which is in good agreement with the previous study. Of 10 hearts with similar ranges of myocardial siderosis, the mean global myocardial iron causing severe heart failure was 5.98 ± 2.42 mg/g dw (range, 3.19 to 9.50 mg/g dw), but in 1 outlier case of heart failure, myocardial iron was 25.9 mg/g dw. The values seen in the 10 hearts are rather modest compared with iron levels commonly seen in the liver in β -thalassemia major, indicating that the heart is considerably more sensitive to iron loading than the liver in terms of functional consequences. The outlier heart had 5 times the iron concentration compared with the mean value of the other hearts, which was a totally unexpected finding. The explanation for this tolerance to myocardial iron can only be speculative, but may have been genetically mediated.

Also of interest is the myocardial T2* value in relation to the development of heart failure and death. Previous ranges for T2* in vivo have been derived solely from clinical observations. In normal volunteers with no history of blood transfusion or iron overload, the first article by Anderson and coworkers⁸ on myocardial T2* found a mean normal value of 52 milliseconds, which yields a myocardial iron concentration of 0.36 mg/g dw from our calibration. More recently, a normal mean value of 40 milliseconds has been widely used, which equates to 0.50 mg/g dw. These values accord well with the previous published normal values for myocardial

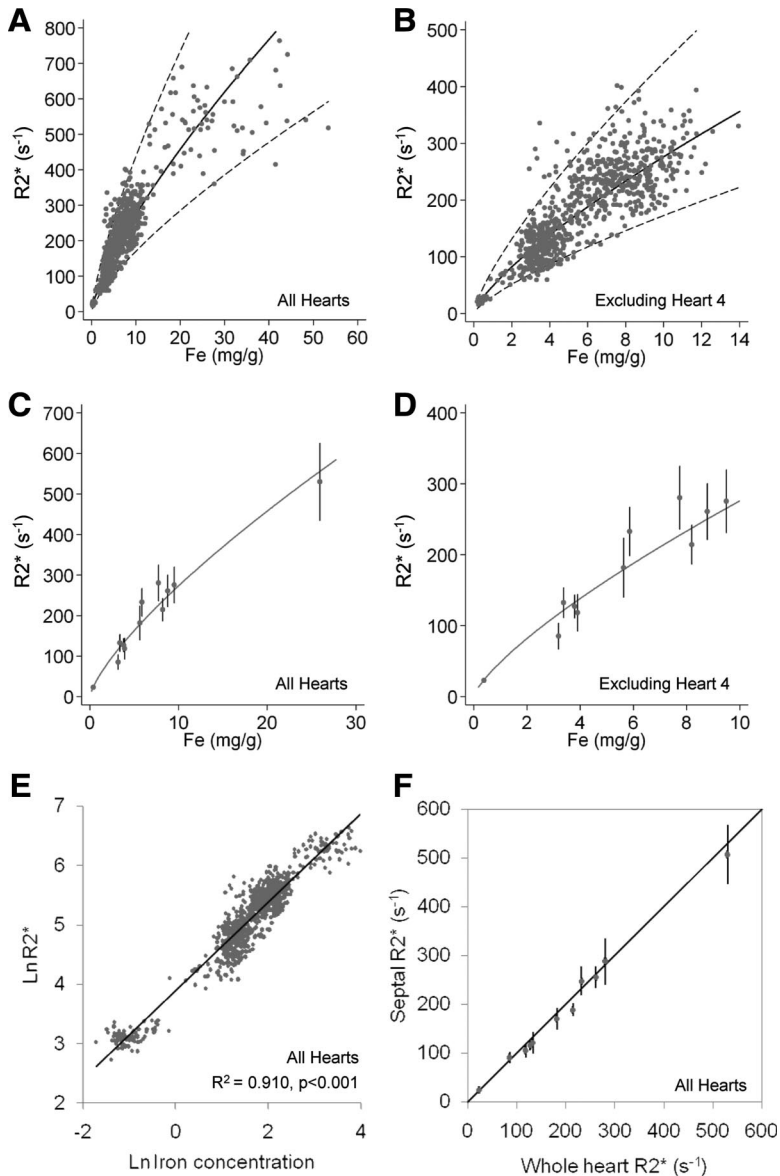


Figure 5. Calibration of cardiac magnetic resonance vs myocardial iron concentration. **A**, $R2^*$ plotted vs myocardial iron concentration measured from each myocardial region of interest (ROI). The regression (solid line) and 95% confidence bands (dotted lines) are shown and derived from analysis of the log-log data shown in **E**. **B**, $R2^*$ vs myocardial iron concentration excluding heart 4. The regression (solid line) and 95% confidence bands (dotted lines) are shown and derived from analysis of the log-log data shown in **E**. **C**, Mean $R2^*$ plotted vs mean iron concentration for each heart. The regression (solid line) is derived from analysis of the log-log data shown in **E**. **D**, Mean $R2^*$ vs mean iron concentration excluding heart 4. The regression (solid line) is derived from analysis of the log-log data shown in **E**. **E**, $\ln(R2^*)$ plotted vs $\ln(\text{Fe})$ for all ROIs, including heart 4, showing the best-fit linear regression line. **F**, Mean midseptal $R2^*$ vs mean whole-heart $R2^*$ plotted against the line of identity showing that the septal $R2^*$ value is highly representative of the whole-heart $R2^*$ (only 11 hearts are shown because severe artifact prevented analysis of midseptal $T2^*$ in 1 heart).

iron³³ and with the global myocardial $T2^*$ value (44.4 milliseconds) of 1 patient in our study who died of a stroke. The myocardial $T2^*$ values associated with being below the normal range are typically <20 milliseconds (1.1 mg/g dw), and as $T2^*$ falls below 10 milliseconds (2.7 mg/g dw), there is a progressive decline in both LV and RV ejection fractions.^{8,34} The vast majority of patients who present with heart failure caused by cardiac iron overload have $T2^* < 10$ milliseconds, and low $T2^*$ values are powerful independent predictors of the subsequent development of cardiac failure.³⁵ All but one of the hearts in this study were from patients who either had died of heart failure or had undergone cardiac transplantation for end-stage heart failure. In keeping with clinical experience, the mean myocardial $T2^*$ was 5.9 ± 3.0 milliseconds (range, 2.0 to 12.3 milliseconds).

Limitations

This project has required international collaboration between specialist centers and could not have been performed with

fresh, unfixed hearts, owing to regulations on transport of human tissue between sites. The fact that death resulting from cardiac failure is almost always restricted to patients with severe cardiac iron loading ($T2^* < 10$ milliseconds) is reflected in the range of $T2^*$ values. Although there is no guarantee that in vivo myocardial $T2^*$ and ex vivo myocardial $T2^*$ are the same, the data are supportive with good agreement between pre-mortem and post-mortem $T2^*$ values in 3 hearts. Some hearts had been stored in formalin over extended periods, but our data suggest that there is no significant change in $T2^*$ over time and only a small amount of leaching of iron into the formalin solution. Although every effort was made to correlate ROIs used for $R2^*$ measurement with the tissue blocks analyzed for iron concentration, it is not possible to eliminate disparity completely. There are difficulties with $R2^*$ measurement in heavily iron-loaded tissue in which signal decay is rapid, requiring very short echo times. Scanner hardware imposes constraints on minimum echo spacing, which may be inadequate for accurate $R2^*$ measure-

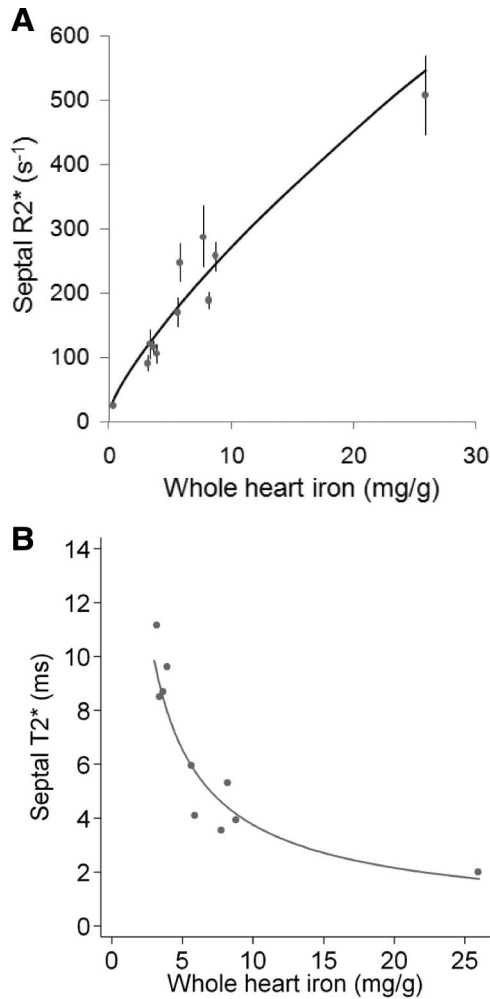


Figure 6. Septal cardiac magnetic resonance measurements vs myocardial iron concentration. **A**, Mean septal R2* plotted against mean iron concentration for each heart. Error bars are \pm SD for septal R2*, and the regression line is based on the log-log data in Figure 5E. **B**, Mean septal T2* plotted against mean iron concentration for each heart. These 2 graphs illustrate the difference between T2* and R2* compared with tissue iron. T2* shortens with increased iron concentration; hence, its reciprocal, R2*, rises with tissue iron. T2* is used for clinical assessment of cardiac iron for historical reasons.

ment at very high iron concentrations. However, a minimum echo time of 1.2 milliseconds should allow reliable measurement of T2* values as low as 1.44 milliseconds,¹⁶ which is below the minimum global myocardial value seen in this study. Finally, some ROIs were excluded from the calibration because of imaging artifact. The decision to exclude an ROI was made by subjective assessment before the analysis of R2* and is unlikely to have affected the calibration significantly, owing to the many regions sampled throughout the 12 hearts. Previous reports have examined the myocardial relaxation parameter T2 in relation to cardiac iron in animal models³⁶ and in humans.^{16,19} T2 imaging can be challenging, however, and it is not in routine clinical use, although recent imaging advances have been made.³⁷ Because of the ease of acquisition and robust nature of T2* for clinical practice, we have concentrated on this technique.

Conclusion

The results of the present study validate the clinical technique in current use and provide detailed calibration and distribution data in humans.

Acknowledgments

We are indebted to the generosity of the patients and families without whose help we would have been unable to perform this important study. We would like to thank Steven Collins for assistance in scanning the ex vivo hearts and Cathleen Enriquez for her assistance in preparing this manuscript.

Sources of Funding

This work was supported by the National Institute for Health Research Cardiovascular Biomedical Research Unit at the Royal Brompton and Harefield National Health Service Foundation Trust and Imperial College London. Financial support was also received from the National Institutes of Health through grant No. R01 DK066084-01, and from the Australian Research Council through grant No. DP0985848.

Disclosures

Dr Carpenter has received honoraria from Novartis, Apotex, and Swedish Orphan. Dr He is supported by the British Heart Foundation and is a consultant to Novartis. Dr Porter has received research funding from and served on the speakers' bureau and advisory board for Novartis. Professor Galanello served on the speakers' bureau for Novartis and ApoPharma. Dr Forni has received research funding from Novartis. Dr Fucharoen is a Senior Research Scholar of the Thailand Research Fund. Dr Firmin has received research support from Siemens. Dr Pennell is a consultant to and has served on advisory boards and speakers' bureaus for Novartis, ApoPharma, and Siemens; has received research funding from Novartis; and is a director and stockholder for Cardiovascular Imaging Solutions. Dr St. Pierre holds shares in and is on the Board of Directors of Resonance Health Ltd and has received research funding from Novartis. Dr Wood has received research funding from Novartis and is a consultant for Ferrokin Biosciences. The other authors report no conflicts.

References

1. Gordeuk VR, Bacon BR, Brittenham GM. Iron overload: causes and consequences. *Ann Rev Nutr.* 1987;7:485–508.
2. McLaren GD. Iron overload disorders: natural history, pathogenesis, diagnosis, and therapy. *Crit Rev Clin Lab Sci.* 1983;19:205–266.
3. Borgna-Pignatti C, Rugolotto S, De Stefano P, Piga A, Di Gregorio F, Gamberini MR, Sabato V, Melevendi C, Cappellini MD, Verlato G. Survival and disease complications in thalassemia major. *Ann NY Acad Sci.* 1998;850:227–231.
4. Modell B, Khan M, Darlison M. Survival in beta thalassaemia major in the UK: data from the UK Thalassaemia Register. *Lancet.* 2000;355:2051–2052.
5. Modell B, Khan M, Darlison M, Westwood MA, Ingram D, Pennell DJ. Improved survival of thalassaemia major in the UK and relation to T2* cardiovascular magnetic resonance. *J Cardiovasc Magn Reson.* 2008;10:42.
6. Borgna-Pignatti C, Rugolotto S, De Stefano P, Zhao H, Cappellini MD, Del Vecchio GC, Romeo MA, Forni GL, Gamberini MR, Ghilardi R, Piga A, Cnaan A. Survival and complications in patients with thalassemia major treated with transfusion and deferoxamine. *Haematologica.* 2004;89:1187–1193.
7. Felker GM, Thompson RE, Hare JM, Hruban RH, Clemetson DE, Howard DL, Baughman KL, Kasper EK. Underlying causes and long-term survival in patients with initially unexplained cardiomyopathy. *N Engl J Med.* 2000;342:1077–1084.
8. Anderson LJ, Holden S, Davis B, Prescott E, Charrier CC, Bunce NH, Firmin DN, Wonke B, Porter J, Walker JM, Pennell DJ. Cardiovascular T2-star (T2*) magnetic resonance for the early diagnosis of myocardial iron overload. *Eur Heart J.* 2001;23:2171–2179.
9. Leonardi B, Margossian R, Colan SD, Powell AJ. Relationship of magnetic resonance imaging estimation of myocardial iron to left ventricular systolic and diastolic function in thalassemia. *J Am Coll Cardiol Cardiovasc Imaging.* 2008;1:572–578.

10. Fitchett DH, Coltart DJ, Littler WA, Leyland MJ, Trueman T, Gozzard DI, Peters TJ. Cardiac involvement in secondary haemochromatosis: a catheter biopsy study and analysis of myocardium. *Cardiovasc Res*. 1980;14:719–724.
11. Olson LJ, Edwards WD, Holmes DR Jr, Miller FA Jr, Nordstrom LA, Baldus WP. Endomyocardial biopsy in hemochromatosis: clinicopathologic correlates in six cases. *J Am Coll Cardiol*. 1989;13:116–120.
12. Westwood MA, Anderson LJ, Firmin DN, Gatehouse PD, Lorenz CH, Wonke B, Pennell DJ. Interscanner reproducibility of cardiovascular magnetic resonance T2* measurements of tissue iron in thalassemia. *J Magn Reson Imaging*. 2003;18:616–620.
13. Westwood M, Anderson LJ, Firmin DN, Gatehouse PD, Charrier CC, Wonke B, Pennell DJ. A single breath-hold multiecho T2* cardiovascular magnetic resonance technique for diagnosis of myocardial iron overload. *J Magn Reson Imaging*. 2003;18:33–39.
14. Kirk P, He T, Anderson LJ, Roughton M, Tanner MA, Lam WW, Au WY, Chu WC, Chan G, Galanello R, Matta G, Fogel M, Cohen AR, Tan RS, Chen K, Ng I, Lai A, Fucharoen S, Laothamata J, Chuncharunee S, Jongjirasiri S, Firmin DN, Smith GC, Pennell DJ. International reproducibility of single breathhold T2* MR for cardiac and liver iron assessment among five thalassemia centers. *J Magn Reson Imaging*. 2010;32:315–319.
15. Wood JC, Enriquez C, Ghugre N, Tyzka JM, Carson S, Nelson MD, Coates TD. MRI R2 and R2* mapping accurately estimates hepatic iron concentration in transfusion-dependent thalassemia and sickle cell disease patients. *Blood*. 2005;106:1460–1465.
16. Wood JC, Otto-Duessel M, Aguilar M, Nick H, Nelson MD, Coates TD, Pollack H, Moats R. Cardiac iron determines cardiac T2*, T2, and T1 in the gerbil model of iron cardiomyopathy. *Circulation*. 2005;112:535–543.
17. Ghugre NR, Enriquez CM, Gonzalez I, Nelson MD Jr, Coates TD, Wood JC. MRI detects myocardial iron in the human heart. *Magn Reson Med*. 2006;56:681–686.
18. Wang ZJ, Fischer R, Chu Z, Mahoney DH Jr, Mueller BU, Muthupillai R, James EB, Krishnamurthy R, Chung T, Padua E, Vichinsky E, Harmatz P. Assessment of cardiac iron by MRI susceptometry and R2* in patients with thalassemia. *Magn Reson Imaging*. 2010;28:363–371.
19. Mavrogeni SI, Markussis V, Kaklamanis L, Tsiapras D, Paraskevaidis I, Karavolias G, Karagiorga M, Douskou M, Cokkinos DV, Kremastinos DT. A comparison of magnetic resonance imaging and cardiac biopsy in the evaluation of heart iron overload in patients with beta-thalassemia major. *Eur J Haematol*. 2005;75:241–247.
20. Cerqueira MD, Weissman NJ, Dilsizian V, Jacobs AK, Kaul S, Laskey WK, Pennell DJ, Rumberger JA, Ryan T, Verani MS. Standardized myocardial segmentation and nomenclature for tomographic imaging of the heart: a statement for healthcare professionals from the Cardiac Imaging Committee of the Council on Clinical Cardiology of the American Heart Association. *Circulation*. 2002;105:539–542.
21. He T, Gatehouse PD, Kirk P, Mohiaddin RH, Pennell DJ, Firmin DN. Myocardial T2* measurement in iron-overloaded thalassemia: an ex vivo study to investigate optimal methods of quantification. *Magn Reson Med*. 2008;60:350–356.
22. Olson LJ, Edwards WD, McCall JT, Ilstrup DM, Gersh BJ. Cardiac iron deposition in idiopathic hemochromatosis: histologic and analytic assessment of 14 hearts from autopsy. *J Am Coll Cardiol*. 1987;10:1239–1243.
23. Engle MA, Erlanson M, Smith CH. Late cardiac complications of chronic, severe, refractory anemia with hemochromatosis. *Circulation*. 1964;30:698–705.
24. Schellhammer PF, Engle MA, Hagstrom JW. Histochemical studies of the myocardium and conduction system in acquired iron-storage disease. *Circulation*. 1967;35:631–637.
25. James TN. Pathology of the cardiac conduction system in hemochromatosis. *N Engl J Med*. 1964;271:92–94.
26. Buja LM, Roberts WC. Iron in the heart: etiology and clinical significance. *Am J Med*. 1971;51:209–221.
27. Kyriacou K, Michaelides Y, Senkus R, Simamonian K, Pavlides N, Antoniadis L, Zambartas C. Ultrastructural pathology of the heart in patients with beta-thalassaemia major. *Ultrastruct Pathol*. 2000;24:75–81.
28. Positano V, Pepe A, Santarelli MF, Ramazzotti A, Meloni A, De Marchi D, Favilli B, Cracolici E, Midiri M, Spasiano A, Lombardi M, Landini L. Multislice multiecho T2* cardiac magnetic resonance for the detection of heterogeneous myocardial iron distribution in thalassaemia patients. *NMR Biomed*. 2009;22:707–715.
29. Pepe A, Positano V, Santarelli MF, Sorrentino F, Cracolici E, De Marchi D, Maggio A, Midiri M, Landini L, Lombardi M. Multislice multiecho T2* cardiovascular magnetic resonance for detection of the heterogeneous distribution of myocardial iron overload. *J Magn Reson Imaging*. 2006;23:662–668.
30. Wacker CM, Bock M, Hartlep AW, Beck G, van Kaick G, Ertl G, Bauer WR, Schlad LR. Changes in myocardial oxygenation and perfusion under pharmacological stress with diprydamole: assessment using T2* and T1 measurements. *Magn Reson Med*. 1999;41:686–695.
31. He T, Smith G, Carpenter JP, Mohiaddin R, Pennell DJ, Firmin D. A phantom study of temperature-dependent MRI T2* measurement. Abstract. *J Cardiovasc Magn Reson*. 2009; 11(suppl 1):P147.
32. Chua-anusorn W, Webb J, Macey DJ, Pootrakul P, St Pierre TG. The effect of histological processing on the form of iron in iron-loaded human tissues. *Biochim Biophys Acta*. 1997;1360:255–261.
33. Collins W, Taylor WH. Determination of iron in cardiac and liver tissues by plasma emission spectroscopy. *Ann Clin Biochem*. 1987;24:482–487.
34. Alpendurada F, Carpenter JP, Deac M, Kirk P, Walker JM, Porter JB, Banya W, He T, Smith GC, Pennell DJ. Relation of myocardial T2* to right ventricular function in thalassaemia major. *Eur Heart J*. 2010;31:1648–1654.
35. Kirk P, Roughton M, Porter JB, Walker JM, Tanner MA, Patel J, Wu D, Taylor J, Westwood MA, Anderson LJ, Pennell DJ. Cardiac T2* magnetic resonance for prediction of cardiac complications in thalassemia major. *Circulation*. 2009;120:1961–1968.
36. Liu P, Henkelman M, Joshi J, Hardy P, Butany J, Iwanochko M, Clauberg M, Dhar M, Mai D, Waien S, Olivieri N. Quantification of cardiac and tissue iron by nuclear magnetic resonance relaxometry in a novel murine thalassaemia-cardiac iron overload model. *Can J Cardiol*. 1996;12:155–164.
37. He T, Gatehouse PD, Anderson LJ, Tanner M, Keegan J, Pennell DJ, Firmin DN. Development of a novel optimized breathhold technique for myocardial T2 measurement in thalassemia. *J Magn Reson Imaging*. 2006;24:580–585.

CLINICAL PERSPECTIVE

Measurement of myocardial iron is key to the clinical management of patients at risk of iron-overload cardiomyopathy, which is a major killer in transfusion-dependent patients and others with errors of iron metabolism. This applies especially to the large cohort of β -thalassaemia major patients, in whom iron accumulation leads to damage in the liver, heart, and endocrine organs. Myocardial iron is assessed clinically with the cardiovascular magnetic resonance relaxation parameter T2*. This study describes the calibration of cardiovascular magnetic resonance relaxation against human iron concentration and the iron distribution throughout the heart under conditions of iron overload. A strong correlation was observed between cardiovascular magnetic resonance relaxation measurements and biochemically derived tissue iron concentration in 12 postmortem human hearts from transfusion-dependent patients, leading to a clinical calibration equation of $[\text{Fe}] = 45.0 \times (\text{T2}^*)^{-1.22}$, where $[\text{Fe}]$ is measured in milligrams per gram dry weight and T2* is measured in milliseconds. There was no systematic variation in iron concentration throughout the heart, but higher iron levels were found in the epicardium than in the endocardium. The data also show that cardiovascular magnetic resonance measurements in the midventricular septum are very representative of whole-heart iron concentration, which validates the current clinical approach in widespread use. These data show that T2* cardiovascular magnetic resonance can be used to measure myocardial iron and validate its use as an end point in clinical trials for the improvement of efficacy of cardiac iron chelation treatment to prevent heart failure and death. This will significantly affect the health care of the many thousands of transfusion-dependent patients worldwide.

On T2* Magnetic Resonance and Cardiac Iron

John-Paul Carpenter, Taigang He, Paul Kirk, Michael Roughton, Lisa J. Anderson, Sofia V. de Noronha, Mary N. Sheppard, John B. Porter, J. Malcolm Walker, John C. Wood, Renzo Galanella, Gianluca Forni, Gualtiero Catani, Gildo Matta, Suthat Fucharoen, Adam Fleming, Michael J. House, Greg Black, David N. Firmin, Timothy G. St. Pierre and Dudley J. Pennell

Circulation. 2011;123:1519-1528; originally published online March 28, 2011;
doi: 10.1161/CIRCULATIONAHA.110.007641

Circulation is published by the American Heart Association, 7272 Greenville Avenue, Dallas, TX 75231
Copyright © 2011 American Heart Association, Inc. All rights reserved.
Print ISSN: 0009-7322. Online ISSN: 1524-4539

The online version of this article, along with updated information and services, is located on the
World Wide Web at:

<http://circ.ahajournals.org/content/123/14/1519>

Permissions: Requests for permissions to reproduce figures, tables, or portions of articles originally published in *Circulation* can be obtained via RightsLink, a service of the Copyright Clearance Center, not the Editorial Office. Once the online version of the published article for which permission is being requested is located, click Request Permissions in the middle column of the Web page under Services. Further information about this process is available in the [Permissions and Rights Question and Answer](#) document.

Reprints: Information about reprints can be found online at:
<http://www.lww.com/reprints>

Subscriptions: Information about subscribing to *Circulation* is online at:
<http://circ.ahajournals.org/subscriptions/>